European Geosciences Union General Assembly 2014, EGU 2014

The deep structure of the Larderello-Travale geothermal field (Italy) from integrated, passive seismic investigations

Gilberto Saccorotti[a,][*], Davide Piccinini[a], Maria Zupo[a], Francesco Mazzarini[a], Claudio Chiarabba[a], Nicola Piana Agostinetti[b], Andrea Licciardi[b,c] and Matteo Bagagli[a]

[a] *Istituto Nazionale di Geofisica e Vulcanologia, Italy*
[b] *Dublin Institute for Advanced Studies, Geophysics Section, Dublin, Ireland*
[c] *University College of Dublin – School of Geological Sciences,Dublin,Ireland.*

Abstract

We report the preliminary results from a project (GAPSS-Geothermal Area Passive Seismic Sources), aimed at testing the resolving capabilities of passive exploration methods on a well-known geothermal area, namely the Larderello-Travale Geothermal Field (LTGF). Located in the western part of Tuscany (Italy), LTGF is the most ancient geothermal power field of the world. GAPSS consisted of up to 20 seismic stations deployed over an area of about 50 x 50 Km. During the first 12 months of measurements, we located more than 2000 earthquakes, with a peak rate of up to 40 shocks/day. Preliminary results from analysis of these signals include: (i) analysis of Shear-Wave-Splitting from local earthquake data, from which we determined the areal distribution of the most anisotropic regions; (ii) local-earthquake travel-time tomography for both P- and S-wave velocities; (iii) telesismic receiver function aimed at determining the high-resolution (<0.5km) S-velocity structure over the 0-20km depth range, and seismic anisotropy using the decomposition of the angular harmonics of the RF data-set; (iv) S-wave velocity profiling through inversion of the dispersive characteristics of Rayleigh waves from earthquakes recorded at regional distances. After presenting results from these different analyses, we eventually discuss their potential application to the characterisation and exploration of the investigated area.

---

* Corresponding author. Tel.: +39-050-8311960; fax: +39-050-8311942.
 E-mail address: gilberto.saccorotti@pi.ingv.it

1. Introduction

Many geothermal areas exhibit higher background seismicity than their surrounding regions, and the potential of such signals as a prospecting tool was first pointed out by [1]. Since then, substantial advances have been made in the development and application of methodologies aimed at reconstructing the distribution of seismological parameters (mostly velocities) at depth. In common with all other geophysical exploratory disciplines, passive seismic methods have both advantages and disadvantages. On the positive side, they can sample rock volumes which would be unreachable otherwise, and they are usually cost-effective as they do not require the utilisation of expensive artificial sources. On the negative side, they usually require long acquisition times, and they do offer a non-uniform imaging of the rock volumes under investigation as a consequence of the uneven distribution of sources. Notwithstanding these limitations, the application of passive seismic methods to the improved understanding of geothermal areas is constantly growing in response to the greater keenness in exploiting geothermal resources.

Within this general context, this paper aims at presenting an integrated application of different, complementary passive seismic methods. Our target is the Larderello-Travale Geothermal Field (LTGF; Italy), whose internal structure is well constrained through direct probing and geophysical exploration, and which is presently the object of renewed exploration programs.

2. Geological outline

The Larderello-Travale geothermal field (Fig. 1) is a large area of the Northern Apennines where, since the Pliocene, the emplacement of shallow-level intrusions has led to the development of diffuse thermal aureoles and associated hydrothermal systems, both sampled by several wells drilled for geothermal exploration and exploitation ([2], [3], [4], [5]). Larderello is a steam-dominated geothermal field whose exploitation dates back to 1905. The whole geothermal area is about 400 km2 and has a production of more than 1000 kg/s of super-heated steam, with a running capacity of about 700 MW [6]. Hydrothermal systems, located at depths ranging between 500 and 4000 m, show an evolution from an early stage, coeval with granitic intrusions, dominated by magmatic and metamorphic fluids, to the present-day stage dominated by meteoric fluids. The growth of hydrothermal mineral assemblages within brittle veins and/or fracture systems is regarded as evidence of fluid circulation coeval with repeated episodes of brittle deformation. The tectonic structure of the geothermal field consists of a stack of Alpine tectonic units, namely the Ligurian Unit and the Tuscan Nappe (Fig. 1), which overlie the Tuscan Metamorphic Complex. The latter is a buried complex of low-grade metamorphic units made up of terrigenous and carbonatic successions of Permian-Triassic [5] and Palaeozoic age rocks [7]. Shallow-level emplacement of Pliocene intrusive rocks in the metamorphic tectonic units led to the development of broad low pressure – high temperature (0.15-0.2 GPa – 500° - 650° C) contact aureoles with development of medium to high grade hornfels rocks and associated hydrothermal systems [3] [4] [5]. A noteworthy feature of the geothermal field is the occurrence of seismic reflectors, named the K-horizon and H-horizon ([8] and references therein). The K-horizon is located at depths in between 3 and 6 km, and it corresponds to the top of the Quaternary granites [7]. This horizon is characterized by a strong amplitude signal of bright-spot type, suggesting the presence of fluids of either magmatic or metamorphic origin hosted within cracks and/or micro-cracks. The K-horizon is thus thought to represent the top of a fluid-rich level [4] [7] that cyclically undergoes episodes of fluid overpressure, as also indicated by concentration of seismic activity [8]. The K-horizon culminates at a depth of nearly 3000 m in the Lago area (south of Larderello; Fig. 1) where the former was reached by the San Pompeo 2 well, which exploded upon reaching the horizon. The overlying H-horizon occurs at shallower depths (2-4 km) in correspondence of the contact aureole of the Pliocene granites and it is regarded as a fossil K-horizon [8]. Main faults in the Larderello geothermal fields are normal faults associated with the latest extensional episode which is lasting since late Pliocene. Faulting affects very shallow crustal levels (about 1 km depth) with major NW-trending, NE-dipping and NE-trending normal to strike-slip steeply dipping fractures [9].
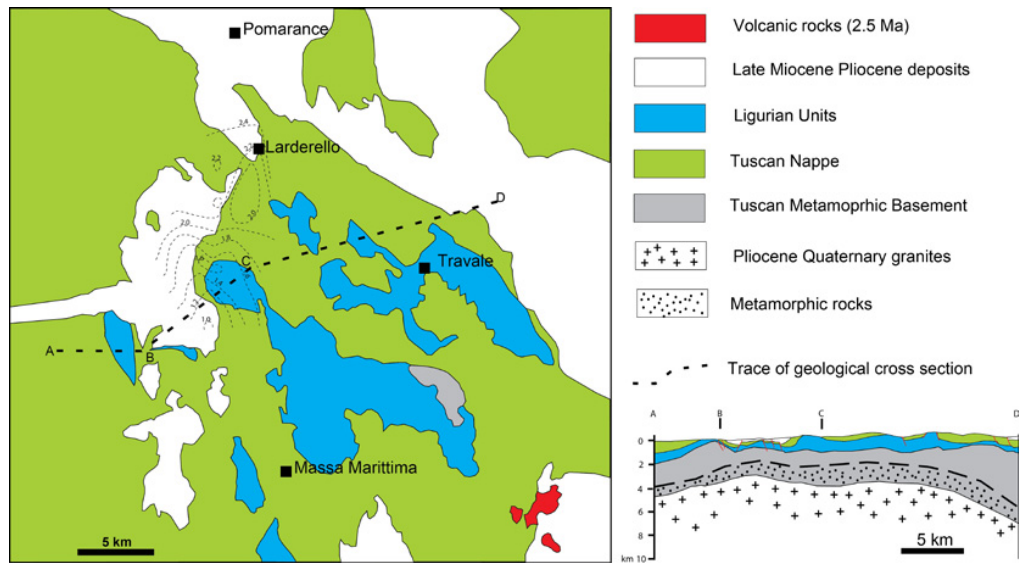
Fig. 1. Geological sketch map of the Larderello-Travale Geothermal field (redrawn after [8]).

3. Data

Data used for this study were gathered in the frame of a specific project (GAPSS - Geothermal Area Passive Seismic Sources), which lasted from early May, 2012, through late October, 2013. It consisted of up to 20 temporary seismic stations deployed over an area of about 50x50 Km, with average station spacing of 10 km. Stations were equipped with either broadband (40s and 120s) or intermediate-period (5s), 3-components seismometers. LTGF is seismically active, and for the the first 12 months of measurements we located more than 2000 earthquakes, with peak rates of up to 40 shocks/day (Fig.2). The largest observed magnitude is M_L=3, and hypocentral depths are generally shallower than 8 km.

4. 4. Analysis

4.1. Travel-time tomography

We inverted P- and S-wave arrival times from local earthquake using the inversion procedure described by [10]. The method uses the finite differences technique to compute theoretical travel times by solving the Eikonal equation through a complex velocity structure and the least squares LSQR algorithm for simultaneous inversion of velocity parameters and hypocenter locations. Also, smoothing constraint equations are used to regularize the solution by controlling the degree of model roughness allowed during the inversion procedure. The 1-D reference velocity model has been obtained using a preliminary 1D inversion. From the initial data set, we selected earthquakes having azimuthal gap smaller than 180°, RMS of time residuals smaller than 1s, and location errors smaller than 0.5km. The selection resulted in 840 events having an average of 10 P- travel-time readings and provided a final dataset consisting of 9680 P- and S-wave arrival times. The distribution of stations/events allowed to investigate a volume of 45 x 30 x 10 km3 with the top at 1 km above the sea level. The investigated volume has been discretised by using uniform velocity cells having size 0.5x0.5x0.5 km^3. Hypocentral depths span the 0-8 km depth range; accurate resolution analyses using both spike and checkerboard tests indicate that velocity anomalies are better resolved at depths shallower than 6 km.

Figure 3 illustrates an EW vertical cross-section of the inverted Vp velocity structure passing through the Travale area.
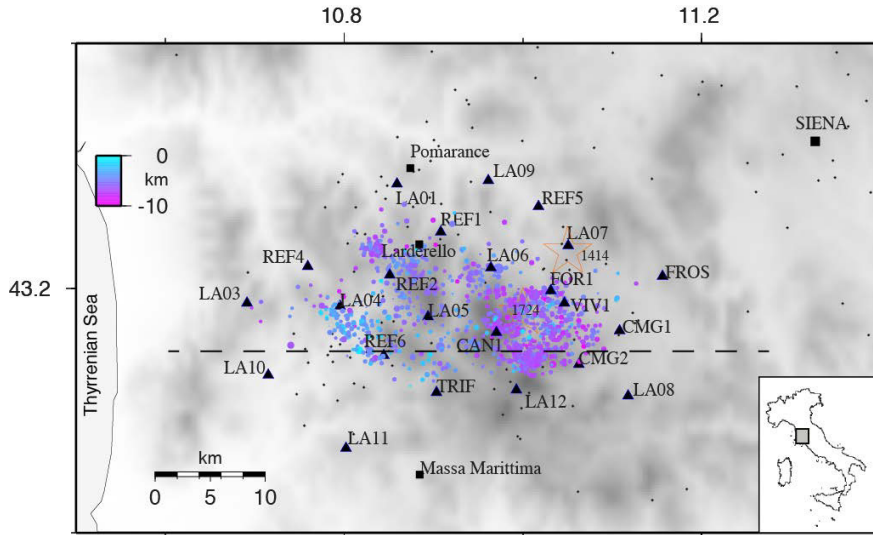
Fig. 2. Map of seismicity recorded during the first three months of the GAPSS experiment (filled, colored circles). The color of the symbols indicate source depth, according to the color scale at the upper left. White dots are those hypocenters located at depths larger than 10 km. Temporary GAPSS stations are marked by black triangles. Dashed line represent the surface trace of the tomographic cross-section in Fig. 3.
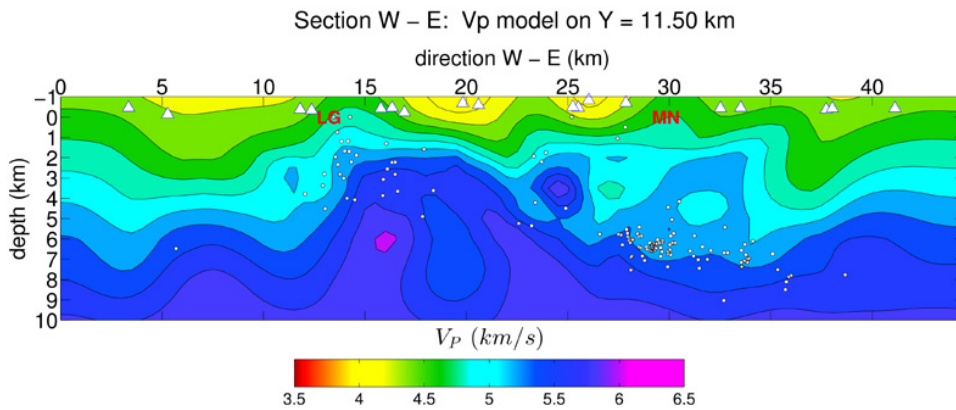

Fig. 3. EW vertical cross-section through the inverted Vp model. The surface trace of this section is indicated by a line in Fig. 2.

The main features emerging from that image are: (i) a dome-like, positive velocity anomaly spanning the central sector of the geothermal field, and (ii) two positive anomalies located in the eastern sector, constituting short-wavelength ripples in the dome-like profile at offsets of about 25 and 32 km into the section. Taken together, the shape of the large- and small-scale anomalies exhibit a striking correspondence with the profiles of the quaternary batholite and Pliocenic granites, respectively, as schematically illustrated in [11]. The top of the deepest, youngest body (i.e., the quaternary pluton) would correspond to the K-horizon, while the upper profile of the two shallowest anomalies (corresponding to the oldest intrusions of Pliocenic age) would mark the H-horizon. This finding is particularly relevant, in light of the fact that this latter horizon is very often associated with fractured, fluid-filled levels, whose detection is of primary importance for the exploitation of the geothermal resource.

4.2. Shear-wave splitting

Shear-wave splitting (SWS) is a powerful passive exploration tool to detect the geometry of fracture system, the intensity of cracking and possibly, changes in fluid pressure within the rock medium. The method is based on the observation that a shear-wave propagating through rocks with stress-aligned micro-cracks (also known as extensive dilatancy anisotropy or EDA-cracks) will split into two waves, a fast one polarized parallel to the predominant crack direction, and a slow one, polarized perpendicular to it [12]. The differential time delay between the arrival of the fast and the slow shear-waves (in the order of few ms) is proportional to crack density [13]. The measurements from the GAPSS recordings are obtained using the method proposed by [14]. Results are suggestive of a pervasive and heterogeneous system of fluid-filled micro fractures. The overall direction obtained stacking the entire dataset composed by 640 SWS estimation indicate a prevalent direction along N120°, coherent with the regional stress field. The maximum delay time reaches a peak of 0.16 s compatible with SWS measurements in neovolcanic zones of Iceland where shear-wave splitting of 0.1–0.3s has been observed [15]
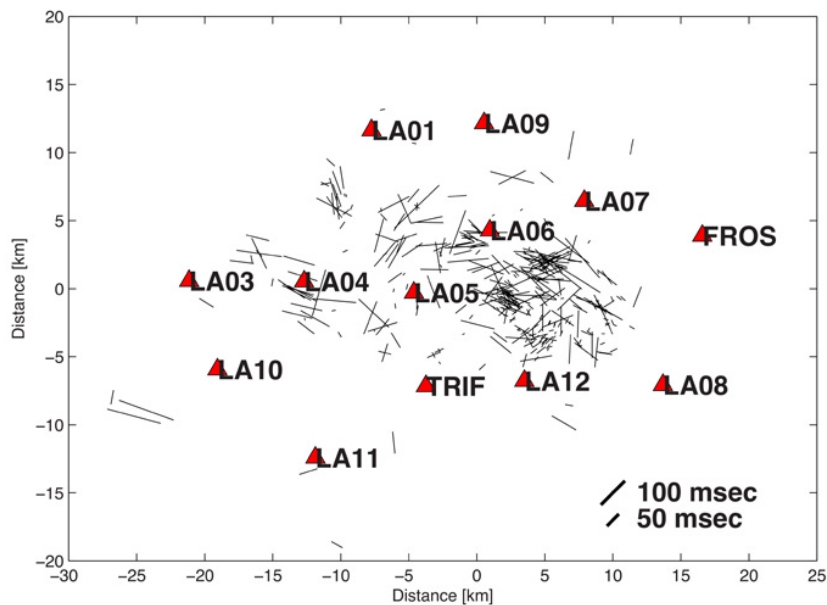

Fig. 4. Distribution of SWS measurements. The orientation of the line segments corresponds to the polarisation direction of the fast S-wave; the length of the lines is proportional to the delay time, according to the scale at the bottom right.

4.3. Surface wave dispersion

Here we analyse the dispersive properties of Rayleigh waves from earthquakes recorded at regional distances, in order to gain clues on the shear-wave velocity profiles. For the analyses we selected 32 earthquakes with magnitudes between 4 and 6, and epicentral distances spanning the 100-200km range. Under the circular wave-front assumption, for each earthquake we calculated velocity-frequency power spectra derived for tentative phase velocities spanning the 2-5 km/s interval. The velocity-frequency power spectra associated with the different earthquakes are then stacked to obtain a single spectrum, whose maxima individuate the fundamental-mode Rayleigh-wave dispersion curve over the 3-20s period range (Fig. 5a). Using a linearised procedure, this curve is then inverted for a shear-wave velocity profile down to 20 km depth (Fig. 5b). The retrieved velocity profile represents an average of the actual S-wave velocity structure beneath the array of stations. Vs varies within a range which is compatible with what derived from earthquake tomography; particularly significant is the low-velocity zone spanning the 5-10km depth range, which could be indicative of the hot rock volumes associated with the most recent granitic intrusion.
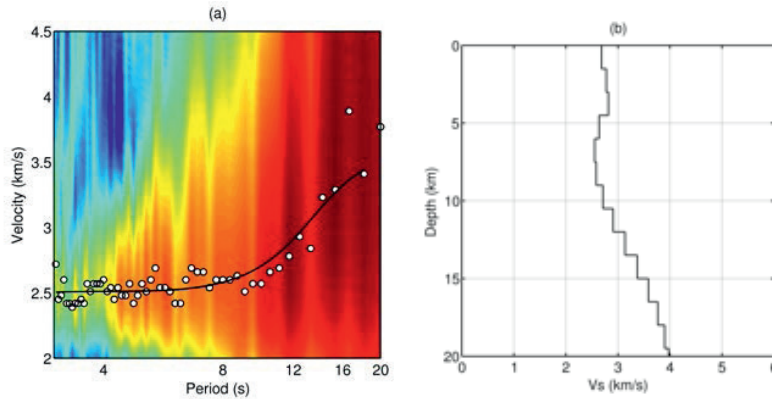
Fig. 5. (a) Velocity-frequency power spectrum derived from stacking of individual spectra from 32 regional earthquakes. Dots indicate the dispersion curve of fundamental-mode Rayleigh waves obtained from the peaks of the power spectrum at individual periods. The black line is the dispersion curve predicted by the velocity structure retrieved by the inversion. (b) Shear-wave velocity structure derived from inversion of the dispersion curve in (a).

4.4. Receiver functions

The Receiver Function (RF) technique is a widely used tool to reconstruct the S-velocity structure beneath a stand-alone broadband seismic station. A teleseismic P-wave is converted into an S-wave as it crosses a velocity discontinuity. The signal generated by each of these conversions is recorded in the P-wave coda and can be extracted from the raw seismic records by deconvolving the vertical-component seismogram from the radial and the transverse ones. The deconvolved signals, called radial and transverse Receiver Function (R-RF and T-RF), represent a time-series of P-to-s (Ps) converted waves. Time-delays between the direct-P, arriving at t=0, and the Ps phases are used to "measure" the depth of the velocity contrast which generated such Ps phases.
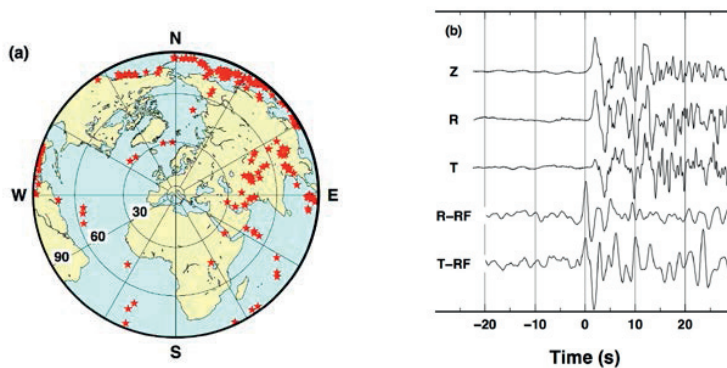

Fig. 6. (a) Epicentral distribution of the teleseisms recorded during the GAPSS experiment (red stars). Numbers dispaly epicentral distance. (b) Examples of teleseismic records and receiver fucntion. Z, R and T labels indicate Vertical, Radial and Transverse component of the P-wave of an earthquakes occured in Iran. R-RF and T-RF mark the Radial and the Transverse receiver function, respectively, obtained from the deconvolution of the Z trace from the R and T traces. Prominent negative phases on the R-RF within the first 3 seconds possibly indicate the occurrence of a low S-velocity zone at depth. The presence of significant energy on the T-RF, in the first seconds, is a marker for anisotropy at shallow crustal depth.

In a perfectly isotropic medium all the conversions due to impedance contrasts at depth are observed in the R-RF while no energy should be present on the T-RF. The presence of anisotropy or dipping interfaces in the subsurface

causes the energy to rotate out of the plane of the incoming wave field and gives a contribution to the TRF with known pattern of variations as a function of the backazimuth [16]. To highlight this effect a good azimuthal distribution of events is required and, depending on the S/N and the quality of the site, this is achieved in at least one year of continuous recording period. Due to the 360°-periodicity of the Ps phases generated by anisotropic layers, the isotropic and anisotropic components of a RF data-set can be decoupled using an harmonic coefficent analysis. In such case, the first harmonics, K=0, contains the contribution from the isotropic structure beneath the station (i.e. the Ps phases generated from discontinuities in the bulk S-velocity profile), while the K=1 harmonics represents the energy of Ps phases converted from anisotropic layers [17].

We computed a RF data-set for each broadband seismic station of the GAPSS experiment. The back-azimuth coverage of the recorded teleseismis is almost completed (Fig. 6a) allowing the analysis of the harmonic coefficients of the RF data-set. High S/N ratio records are selected to computed an average of about 80 RF for each station (Fig. 6b). Overall, a number of RF data-set present prominent negative phases on the R-RF in the first 2 seconds (Fig. 7) indicating in the presence of a low S-velocity zone in the first 0-10 km in the area. Energy in the K=1 harmonics, in the first 2 seconds, suggests anisotropy within the shallow crust.

We modelled the RF data-set using a widely-known forward code [18]. The first 4km of the crust are modelled using the litho-stratigraphy of Sasso 22 borehole. The presence of a negative phase in the first seconds of the K=0 harmonics is reproduced using a S-wave velocity inversion at about 8km depth. The pattern in the K=1 harmonics can be reproduced introducing two anisotropic layers at 5 and 10 km depth (Fig. 7).
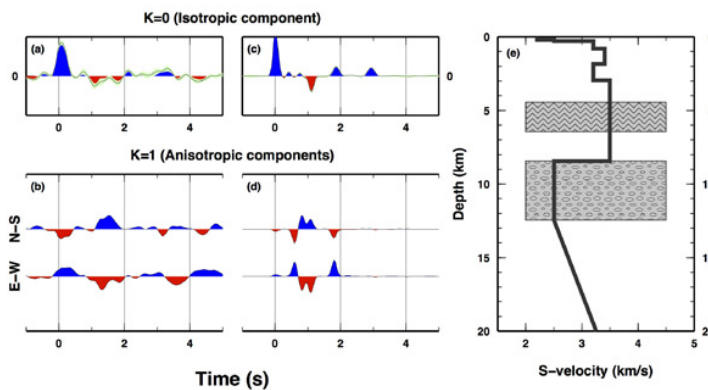

Fig. 7. Observed and synthetic RF for station LA05. (a-b) Observed K=0,1 coeffcents of the harmonic decomposition of the RF data-set. K=0 coefficient represents the P-to-S conversion due to S-velocity discontinuities. The K=1 coefficients shows conversion generated from anisotropic zones at depth. (c-d) synthetic K=0,1 coeffcents of the harmonic decomposition of a RF data-set generated using the model in (e). (e) S-velocity profile used to generate the RF in (c-d). Grey-textures indicate the anisotropic zones at depth which generates the conversion recorded on the K=1 coefficients.

5. Discussion and conclusions

In this work we presented the preliminary results from different analyses carried out on a passive seismological data set collected at the Larderello-Travale Geothermal Field (Italy). Overall, the results obtained thus far exhibit a reasonable correlation with the main geo-structural features of the area as established by previous, independent exploration surveys. While providing a good spatial resolution and information on both Vp and Vs structures, Local Earthquake Tomography is strongly limited by the shallow distribution of hypocenters, which implies lack of illumination for crustal blocks deeper than 4-6 km. Nonetheless, the interpretation of Vp anomalies appears to be well correlated with the inferred location of the H-marker, which generally corresponds to the metamorphic aureole produced by the Pliocenic granitic intrusions. This marker is very often associated with the presence of fractured and permeable levels related to the granite emplacement [11], and it currently represents the principal exploration target in the area.

Additional clues on the location of rock volumes mostly affected by fracturing are provided by analysis of shear-wave splitting. In this case, the areas of intense crustal damage are well individuated by large (>0.1s) delay times, and polarisations of the fast S-wave which depart significantly from the NW-SE trend which is expected once accounting for the regional stress field alone. Within this framework, next steps will aim at refining location and depth of the most significant anisotropic rock volumes, by attempting a 3D inversion of the SWS measurements [19].

Insights into the deeper roots of the geothermal fields are obtained through the inversion of Rayleigh-wave dispersion characteristics and receiver function analysis from earthquakes recorded at regional and teleseismic distances, respectively. By analysing wavelenghts spanning the 3-70 km range, these two latter methods can resolve km-size features over the 0-20 km depth interval. From these analyses, we found a main anisotropic layer at depths around 5 km, and a significant inversion of the Vs gradient over the 8-12km (receiver function) or 5-10km (surface wave inversion) depth intervals.

Future efforts will aim at reconciling all these different findings into a coherent image of the volumetric distribution of compressive and shear-wave velocities beneath the LTGF. Subsequent evaluation of the sensitivies of the investigated seismological parameters for site-relevant rocks under specific physical conditions, will hopefully contribute to an improved imaging of the field in terms of the reservoir rock physical properties, such as fluid content and porosity.

References

[1] Ward, P. L.. Microearthquakes: prospecting tool and possible hazard in the development of geothermal resources. Geothermics 1972; 1, 3 – 12.

[2] Gianelli, G., Manzella, A. and Puxeddu, M. Crustal models of the geothermal areas of southern Tuscany (Italy). Tectonophysics, 1997; 281, 221–239

[3] Carella, M., Fulignati, P., Musumeci, G. and Sbrana, A. Metamorphic consequences of Neogene thermal anomaly in the northern Apennines (Radicondoli – Travale area, Larderello geothermal field, Italy). Geodinamica Acta, 2000; 13, 345–366.

[4] Gianelli, G. and Ruggieri, G., 2002. Evidence of a contact metamorphic aureole with high-temperature metasomatism in the deepest part of the active geothermal field of Larderello, Italy. Geothermics, 31, 443–474.

[5] Musumeci, G., Bocini, L. and Corsi, R.. Alpine tectonothermal evolution of the Tuscan Metamorphic Complex in the Larderello geothermal field (northern Apennines, Italy). Journal of the Geological Society, London, , 2002; 159, 443-456, doi:10.1144/0016-764901-084.

[6] Cappetti, G., Ceppatelli, L.. Geothermal power generation in Italy: 2000–2004 update report. In: Proceedings 2005 World Geothermal Congress, Antalia, Turkey.

[7] Batini, F., Bertini, G., Gianelli, G., Pandeli, E. and Puxeddu, M.. Deep structure of the Larderello field: contribution from recent geophysical and geological data. Soc. Geol. Ital. Mem., 1983; 25, 219–235.

[8] Bertini, G., Casini, M., Gianelli, G. and Pandeli, E. Geological structures of a long-living geothermal system, Larderello, Italy. Terra Nova, 2006; 18, 163–169, doi:10.1111/j.1365-3121.2006.00676.x.

[9] Brogi, A., Lazzarotto, A., Liotta, B. and Ranalli, G. Extensional shear zones as imaged by reflection seismic lines: the Larderello geothermal field (central Italy). Tectonophysics, 2003; 363, 127–139.

[10] Tryggvason, A., S.Th. Rögnval e O.G. Flovenz. Three-dimensional imaging of the P- and S-wave velocity structure and earthquake locations beneath Southwest Iceland. Geophysical Journal International, 2002; 151, 848–866.

[11] M. Casini, S. Ciuffi, A. Fiordelisi and A. Mazzotti. 3D Seismic Surveys and Deep Target Detection in the Larderello-Travale Geothermal Field (Italy). Proceedings World Geothermal Congress 2010 Bali, Indonesia, 25-30 April 2010

[12] Crampin, S. A review of wave motion in anisotropic and cracked elastic media. Wave Motion, 1981; 3, 343–391.

[13] Crampin, S. Geological and industrial implications of extensive dilatancy anisotropy. Nature, 1987; 328, 491–496.

[14] Piccinini, D., M. Pastori, and M. Margheriti. ANISOMAT+: An automatic tool to retrieve seismic anisotropy from local earthquakes *Comput. Geosci.*, 2012; **56**, 62–68, ISSN 0098–3004, doi:10.1016/j.cageo.2013.01.012.

[15] Menke, W., Brandsdóttir, B., Jakobsdóttir, S., Stefánsson, R. Seismic anisotropy in the crust at the mid-Atlantic plate boundary in south-west Iceland. Geophys. J. Int., 1994; 119, 783–790.

[16] Levin, V. and J. Park, P-SH conversions in layered media with hexagonally symmetric anisotropy: A cookbook ,*PAGEOPH*, 1998; 151, 669-697.

[17] Bianchi, I., J. Park, N Piana Agostinetti and V. Levin, Mapping seismic anisotropy using harmonic decomposition of Receiver Functions: an application to Northern Apennines, Italy; Journal of Geophysical Research, 2010; 115, B12317.

[18] Frederiksen and Bostock, 2000 -- Frederiksen, A.W., and Bostock, M.G. Modelling teleseismic waves in dipping anisotropic structures. Geophysical Journal International, 2000; 141 401-412

[19] J.H. Johnson and M.K. Savage, Tracking volcanic and geothermal activity in the Tongariro Volcanic Centre, New Zealand, with shear wave splitting tomography. Journal of Volcanology and Geothermal Research, 2012; 223-224, 1–10.